IEEE Access
Multidisciplinary ⋮ Rapid Review ⋮ Open Access Journal

Received 20 December 2024, accepted 7 January 2025, date of publication 20 January 2025, date of current version 29 January 2025.
Digital Object Identifier 10.1109/ACCESS.2025.3532207

RESEARCH ARTICLE

The Effect of Magnetization on the Production Process of Soft Magnetic Composite Stators of Axial Flux Motors

EMIR POŠKOVIĆ[1], (Member, IEEE), FAUSTO FRANCHINI[2], ELISA FRACCHIA[3], SILVIO VASCHETTO[1], (Senior Member, IEEE), LUCA FERRARIS[2], (Member, IEEE), AND ALBERTO TENCONI[1], (Senior Member, IEEE)
[1]Energy Department, Politecnico di Torino, 10129 Turin, Italy
[2]Energy Department, Politecnico di Torino, 15121 Alessandria, Italy
[3]Department of Management and Production Engineering, Politecnico di Torino, 10129 Turin, Italy

Corresponding author: Emir Pošković (emir.poskovic@polito.it)

The work of Emir Pošković was supported by the FSE REACT-EU-PON Ricerca e Innovazione 2014–2020 within the framework of Ministerial Decree under Grant 1062/2021.

ABSTRACT Axial flux offer a promising and reliable solution for various applications. The use of soft magnetic composite (SMC) materials allows to resolve some of the challenges associated with these motors. Two axial flux motors with identical designs are devolved, with the only variation being in the preparation of the SMC stators. The effect of magnetization during the stator manufacturing process has been assessed. Various tests are conducted in order to compare the performance of the magnetized and non-magnetized stators. Distinct differences have been noted, showing some advantages for the prototype with aligned SMC material. These results are further explained through microstructural analyses.

INDEX TERMS Axial flux motor, soft magnetic composite, magnetization, hysteresis torque, cogging, iron losses, efficiency, microstructural analyses.

I. INTRODUCTION

Axial flux motors are brushless devices that feature unique magnetic orientations in contrast to radial motors [1]. These machines are notable for their compact form and low weight-to-volume ratio. Their high efficiency and simple rotor construction make them ideal for various industrial applications, particularly in the automotive, aerospace, and domestic fields [2], [3], [4], [5], [6], [7]. Furthermore, axial machines can be designed with multiple stator-rotor stages [8], [9]. However, using a single rotor-stator setup can lead to mechanical imbalances, while employing multiple stages can help mitigate this problem. Another drawback is the axial force produced by permanent magnets [10], [11], which requires specialized bearings and makes it more difficult to achieve a very narrow air gap.

The associate editor coordinating the review of this manuscript and approving it for publication was Qinfen Lu.

A proper choice of the magnetic materials plays a fundamental role in the design of axial flux machines, particularly for what concerns their final efficiency [12], [13].

In the selection of permanent magnets, a common solution is represented by sintered NdFeB, due to their high energy density, while sintered ferrites represent a valid alternative, especially for their reduced cost. It must be pointed out that sintered magnets, in particular ferrites, are brittle, and it should become difficult to obtain designs with significant curvature [14]; on the other hand, bonded magnets should be realized in customized shapes thanks to their high machinability [15].

The choice of soft materials to realize the magnetic circuit follows different ways and difficulties to be faced [16], [17]. In traditional machines the choice normally falls on magnetic steels, as they present high magnetic and energetic characteristics up to medium supply frequency, together with high mechanical performance. When dealing with the design of an axial flux machine, the particular shape of the motor stator should represent a significative obstacle if the realization has to be done with laminated steel; an exception should be represented in those cases where the stator poles are realized with U-shaped laminated steel cores [18], with a reduction of the manufacturing cost. Anyway, the realization of such stator cores, in particular the complex punching, is expensive and adopted just for some particular applications, such as sport vehicles and aerospace [19], [20], [21], [22].

An alternative always more frequently adopted is represented by Soft Magnetic Composite (SMC) materials [23], [24], made by ferromagnetic grain powders insulated with organic or inorganic layers, providing significant improvements in terms of material properties, particularly under the thermal and mechanical point of view [25]. The possibility to directly start from the powder makes evident the main advantage of adopting such solution: the realization of complex magnetic geometries is obtained by punching the powder in proper molds. Moreover, as almost each grain is insulated, SMCs present reduced eddy current losses when operating at medium-high frequency compared to traditional laminated steels. They also present isotropic magnetic behavior, making possible to drive the flux in any direction thus simplifying the production of axial flux stators avoiding those magnetic short circuits which typically affect stators realized with laminations.

On the other side SMCs can be criticized for the relatively weak mechanical properties, but under this point of view a significant research activity is being carried out to improve such properties and make these materials capable to be adopted in the challenging realization of axial flux machines stators [26], [27], [28].

The paper deals with the opportunity of applying an external magnetic field to the SMC powder while it is being pressed in the mold and assess the effectiveness of such process. The already underlined isotropic behavior of the SMCs (3D magnetic lines) allows to consider the magnetization to be applied in different directions while punching: axial, radial and orthogonal.

The present work has been organized to compare two different fractional power axial flux machines, where the only difference is represented by the procedure of the stator SMC realization. One stator has been manufactured with a traditional compression molding procedure, while the other one has been realized with the application of a magnetic field during the molding phase. The applied magnetic field has been axially oriented with respect to the punching process direction. The expected results regard an improvement of the stator general properties, both magnetic and energetic, and the validation will be made by means of several electric and mechanical tests on the two prototypes of axial flux machines [29], together with a metallographic analysis of the material.

II. MATERIALS SELECTION

As well known, the first stage in order to select a suitable magnetic material for a specific application is the material selection, whether soft or hard magnets. In this work, permanent magnet samples and SMC samples are produced through laboratory facilities by compression molding.

Concerning the machine rotor, permanent bonded magnets NdFeB have been manufactured and then utilized. In the stator core, a novel specific SMC material was utilized. Such a SMC material was specifically designed for this application that is made up of a hybrid layer consisting of organic and inorganic materials. Mainly, the NdFeB specimens were produced through compression molding at a pressure of 600 MPa. The MQP 14-12 magnetic powder has been used to produce bonded magnets: such powder is currently utilized in applications that requires high temperatures, up to 150 °C. More specifically, a selected epoxy resin has been chosen as the polymeric binder, with a weight content equal to 1% wt. After the blending phase and compacting, the curing process was conducted in a laboratory furnace at 150 °C for 6 hours. The magnet fabricated is featured by the demagnetization curve displayed in Fig. 1: J value represents the magnetic polarization (the typical intrinsic value of the magnet), while B, the magnetic induction, shows magnetic behavior in the presence of the air gap.

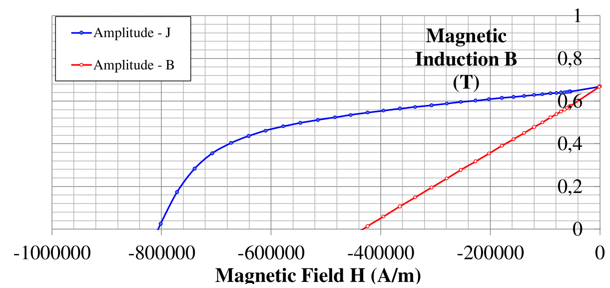

FIGURE 1. Demagnetization curve of bonded magnets prepared by 1 wt.% of epoxy resin.

The production process for the SMC materials was conducted through laboratory facilities thanks to an innovative coating method studied and designed by the Authors [30], [31]. With this method, it is possible to obtain multifunctional nanometric layers by combining diverse materials. The SMC layers here suggested, are obtained by combining polymer and clay, attaining a better producible Soft Magnetic Composite.

The layer-by-layer process (LbL) was here utilized to produce such hybrid layers, utilizing organic and/ or inorganic components in solution baths. Positively charged baths and negatively charged baths are used alternately on the ferromagnetic powder selected up to obtain an adhesion of components on the powders' surface. Each deposition process is followed by a wash-step performed through deionized water. The excess of solution, or the deionized water, is removed by separating the powder from the solution using centrifugal forces and/ or magnetic separation.

Overall, those steps are in the same number as the layers to be realized, while after the last deposition step, the coated powder undergoes a drying process in a vacuum oven at 80 °C [30], [31]. The sketch Fig. 2 highlights the main steps included in the deposition process.

The SMC produced for this work consists of a three-step deposition. Two deposition steps are based on the branched polyethyleneimine polymer applied in water solution, 0.5% in weight of organic material, while the third is based on the montmorillonite clay used in solution 1 wt.%. Notably, mechanical properties for such SMC were measured, obtaining a mechanical strength after the TRS test of about 100 MPa, while as thermal resistance regard, the layers permit a maximum operative temperature of about 300 °C. Magnetic properties of the produced SMC will be discussed later in Section IV.

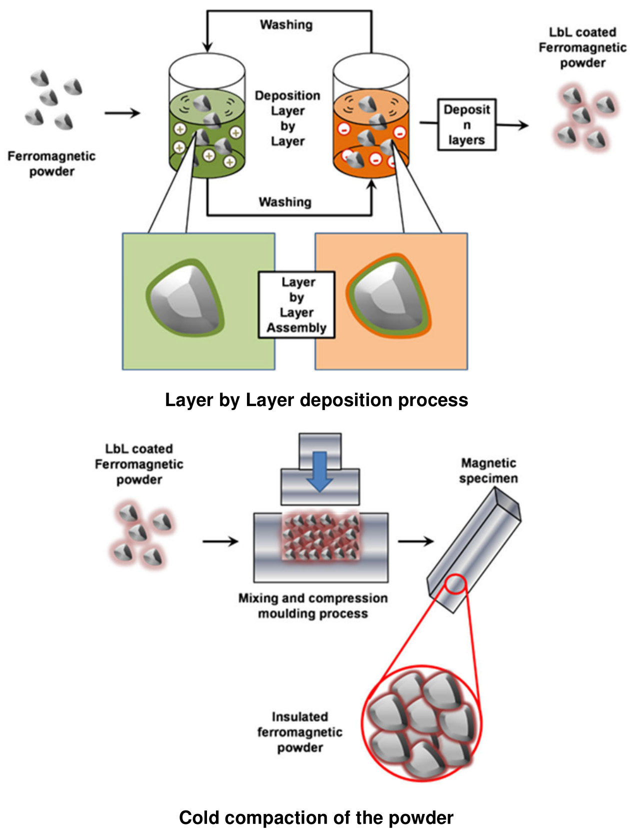

FIGURE 2. Description of the proposed LbL deposition process, from ferromagnetic powder to the final coating magnetic product.

III. PROTOTYPES PREPARATION

Table 1 reports the main axial flux motor data selected through an analytical model based on cyclic interaction, starting from the main parameters, which are the external diameter, the rated torque, the bus voltage and the properties of the designed material, as previously exposed in [10]. Two prototypes of Axial Flux Motor (AFM) were realized using the proposed design of Fig. 3, starting from the same rated conditions and dimensions. Such constraints of the same rated conditions and dimensions are functional to the evaluation of the magnetization effects in SMC materials.

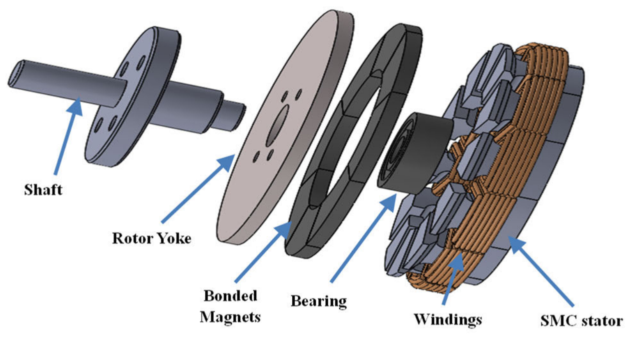

FIGURE 3. Main motor components design.

TABLE 1. Axial flux motor data.

Number of pole pairs	4
Number of slots	12
Motor height	20.7 mm
Stator outer diameter	45 mm
Stator inner diameter	29.7 mm
Rotor outer diameter	45 mm
Rotor inner diameter	29.7 mm
Airgap	0.4 mm
Bus Voltage	12.5 V
Rated speed	4500 rpm
Rated current	1.98 A
Rated torque	60 mNm

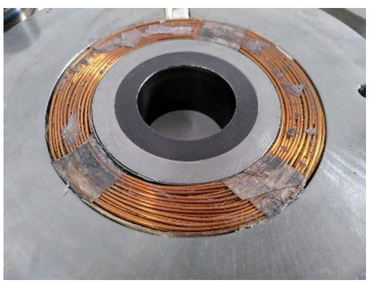

FIGURE 4. The assembly phases of magnetization coil: non-magnetic mold with the turns.

A non-magnetic mold, purposely made for this application, was designed and produced to perform the compression molding process. Conversely, the punches are realized in a magnetic alloy and coated to increase their surface hardness. Stator cores are produced using a pressure of about 500 MPa to obtain compacted cylinders with the design height. During the compression molding, a dedicated magnetization coil built-in into the mold was used to magnetize the powders, as depicted in Fig 4. Fig. 5 shows the compaction phase and the punch.

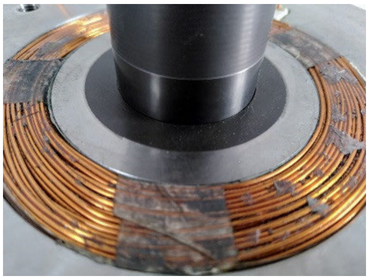

FIGURE 5. The compaction phase: dedicated punch and mold with magnetization coil.

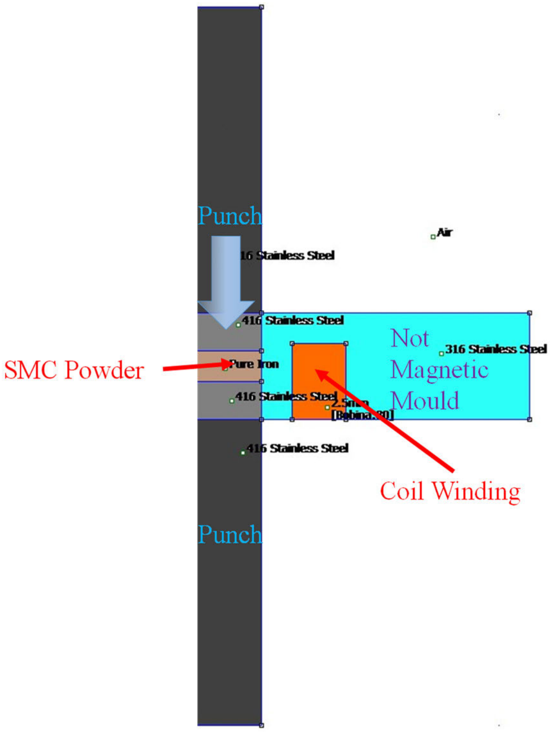

FIGURE 6. Model of compression molding system with the applied magnetization: the punches are ferromagnetic, and the mold size represents the filling level of SMC powder corresponding to the initial chamber height.

A simulation model of such system made possible to predict a flux density over 1 Tesla (for a current pulse of 75 A) where the material to be compacted is placed. On the other hand, the DC supply system at disposal can guarantee a maximum pulsed current of 50 A; anyway, for safety reasons, the applied current is 27 A at 50 V.

The magnetic induction values in the mold can be estimated only with finite element analysis. In fact, the use of a gaussmeter can be considered; on the other hand, it can only provide information about the magnetic flux density into the air gap. Therefore, gaussmeter values can only be used to validate the finite element method. The model for the compaction and magnetization phase is summarized in Fig. 6. By the finite element analyses were performed three simulations, to evaluate the key parameters:

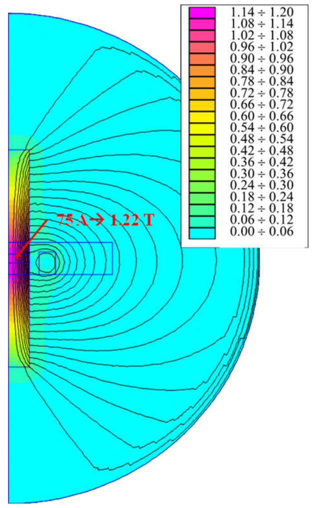

FIGURE 7. Model at the maximum current for magnetization coil cooled in the air (75 A).

- maximum current for magnetization coil cooled in the air, 75 A;
- maximum current for the supply device, 50 A;
- current at safe operation, 27 A.

Finite element simulation permits the assessment of the operative condition related to the magnetization during the production of the SMC stator. Particularly, the simulation in Fig. 7 clearly shows that if the applied current is 75 A, the mold filled with powder is characterized by a flux density of 1.22 T. From the figure, it can be noticed that the magnetic zones extend far beyond the punches area. Similarly, if the applied current is 50 A, as shown in Fig. 8, the flux density in the middle of the mold reaches 0.82 T. Instead, applying a current of 27 A leads to a uniform flux density state inside the mold and a satisfying flux density that can reach 0.44 T, as simulated in Fig. 9. This last analysis corresponds to the selected configuration used to prepare the SMC stator and the experimental tests.

Once the discoidal samples are compacted, the manufacturing of the stators begins. Fig. 10 depicts the production steps. Stators were milled to obtain the final required shape, while the windings of the stator poles are manufactured with 40 turns. The stator windings are wrapped on the stator poles, owing to particular support to facilitate and repeat the winding process similarly. The air gap can be regulated by acting on the bearing positioning using a crew locking system, while the rotor yoke has been realized with an iron plate equipped with bonded magnets. Fig. 11 shows the assembled final motor.

While the rotor is the same for both prototypes, the stator changes as a function of the adoption of the magnetization during the compaction. One stator was manufactured using a discoidal sample compacted with the application of a magnetic field produced by the magnetization coil (configuration Mag-SMC Stator). A second stator was instead manufactured using a compacted sample without

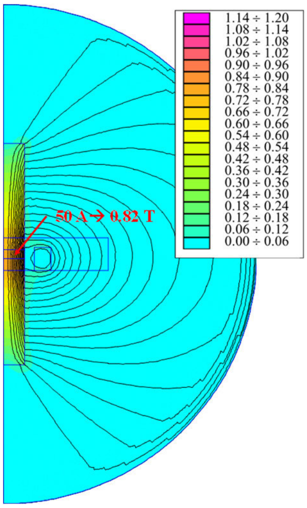

FIGURE 8. Model at maximum current for the supply device (50 A).

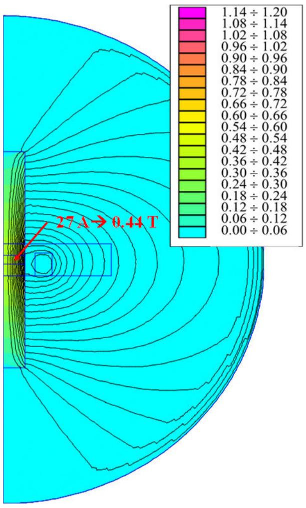

FIGURE 9. Model work at the safe operation (27 A).

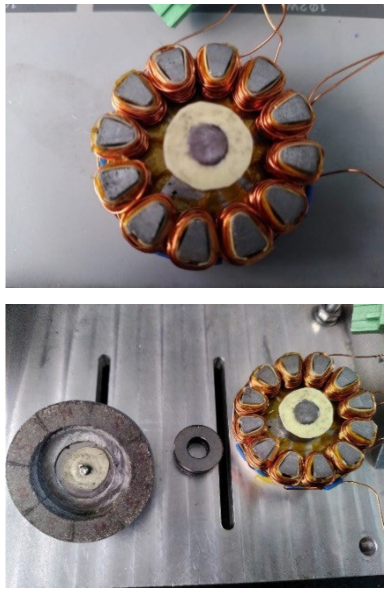

FIGURE 10. Different steps of SMC stator and motor preparation: stator winding, rotor with bonded magnets, and bearings.

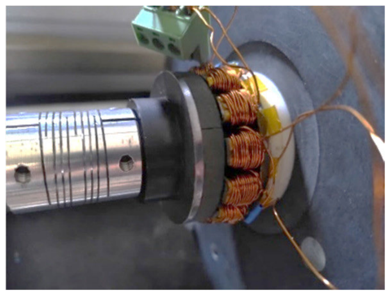

FIGURE 11. The final motor geometry.

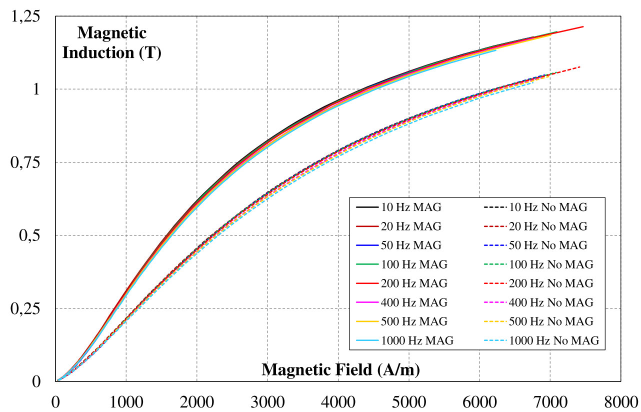

FIGURE 12. BH curves for magnetized and no magnetized SMC materials during the compacted process.

the application of the magnetization (configuration No-Mag SMC Stator).

IV. EXPERIMENTAL RESULTS

Prototypes were tested to assess the effect of applying magnetization on SMC during compaction. Prototypes' responses in terms of the function of the stator material and motor performance were studied, and the results were compared to define the appropriate solution.

A. EFFECT OF MANUFACTURING MAGNETIZATION ON MAGNETIC CHARATERIZATION OF SMC MATERIALS

The obtained SMC materials have been characterized, for what concerns their magnetic properties, on toroidal samples. The characterization method is based on the well-known ''transformer approach''; two windings are wounded around the toroidal magnetic core: the first provides magnetization to the core with a magnetic field H proportional to the current, and the second winding, designed with a very thin copper wire correctly wrapped very close to the magnetic core, detects the induced voltage, proportional to the magnetic flux density B.

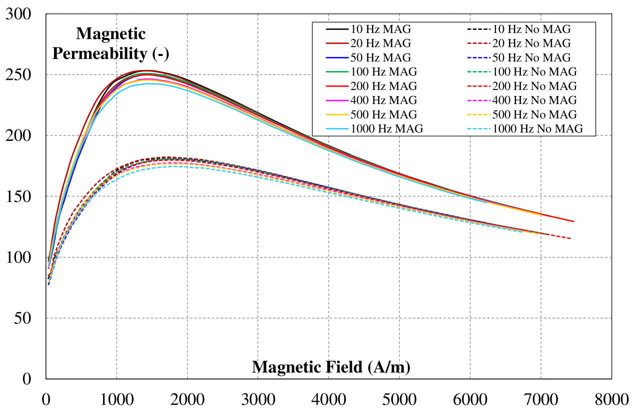

FIGURE 13. Magnetic permeability for magnetized and no magnetized SMC materials during the compacted process.

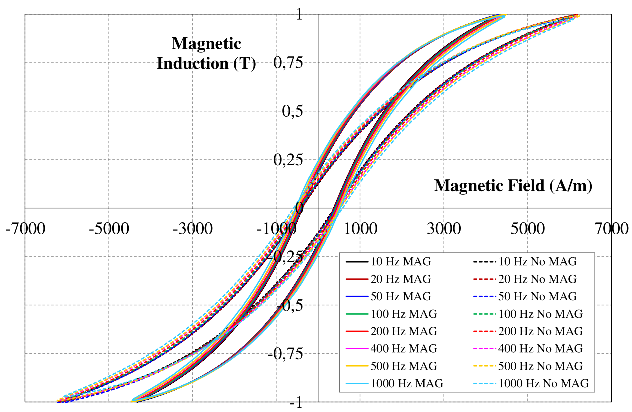

FIGURE 14. Hysteresis loops at 1 T for magnetized and no magnetized SMC materials during the compacted process.

Fig. 12 highlights the resulting characteristics of the B(H) curves in the interval from 10 Hz to 1 kHz as frequency values for both types of SMC compacted samples. Primarily, an important consideration must be done: the B(H) curves in the present work resulted in lower values with respect to typical B(H) curves. This behavior is simply caused by the compaction pressure exerted by the punch, which normally is set to 700÷800 MPa, while for these specific SMC samples, results of about 500 MPa.

From the B(H) curves analysis, one can argue that there is a clear effect of the application of magnetization during the compaction step. Notably, configuration Mag-SMC Stator, namely the configuration with the applied magnetization, led to realize SMC having B(H) curves with large values. In this context, for the same magnetic field, the magnetic induction resulted in higher values in magnetized SMC: at 5000 A/m, 1.05 T was measured in magnetized SMC and 0.9 T in non-magnetized SMC.

SMC specimens magnetized and non-magnetized were even analyzed in terms of magnetic permeability, as in Fig. 13, and also in terms of hysteresis loops, showed in Fig. 14. As magnetic permeability regards, one can analyze curves in Fig. 13 highlighting that the SMC produced with magnetization coil reached a value of about 253, that surprisingly resulted in 40 % higher than SMC produced without magnetization coil (non-magnetized sample). The same results were additionally noticed in hysteresis loops, where the dotted loops highlight the non-magnetized SMC behavior. From observing the cycles, it is evident that SMC non-magnetized has slightly larger cycles than magnetized SMC, resulting in better performances and lower hysteresis losses of the latter.

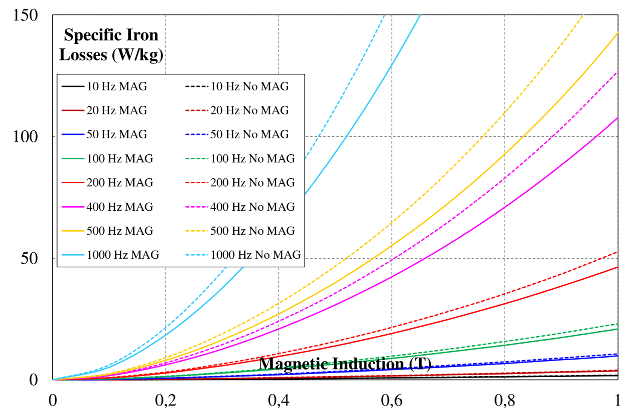

FIGURE 15. Specific iron losses at 1 T for magnetized and no magnetized SMC materials during the compacted process.

Indeed, Fig. 15 shows details about the iron losses in the two SMCs at 1 T. These results permit to assess a clear tendency in terms of iron losses at specific frequencies, confirming a higher value of iron losses in non-magnetized SMC, depicted by the dotted lines in the figure. In other words, one can assess the better performances of the magnetized SMC, even in terms of specific iron losses.

To summarize, all the information obtained from the magnetic characterizations demonstrated clear benefits in applying magnetization during the SMC compaction. The subsequent tests on the prototype were made using the machine with a stator produced without the SMC magnetization during compaction or with the magnetization, aiming to highlight the same trend observed during the materials testing.

B. EFFECT OF MANUFACTURING MAGNETIZATION ON PROTOTYPES: NO-LOAD TEST

The first test that must be performed on prototypes is the no-load test. More in-depth, in this test, the machine is started up without any load, to evaluate the no-load torque and the losses of the machine. In particular, the prototype with magnetized stator showed lower losses and torque, as noticeable from Fig. 16 and Fig. 17; as the mechanical adopted system is the same for both machines, the only difference is depending on the iron losses, resulting lower in the magnetized stator. At 4000 rpm, the prototype with magnetized stator behaved

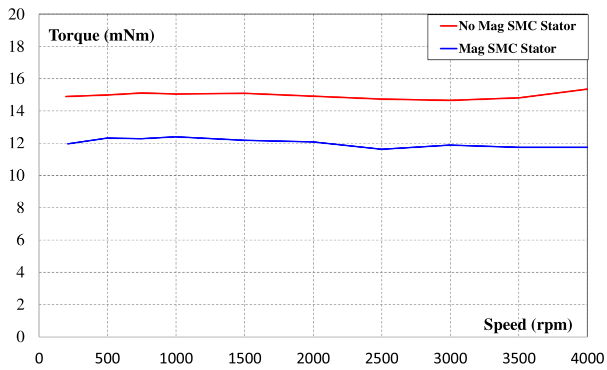

FIGURE 16. No-load test torque measurement for the proposed prototypes.

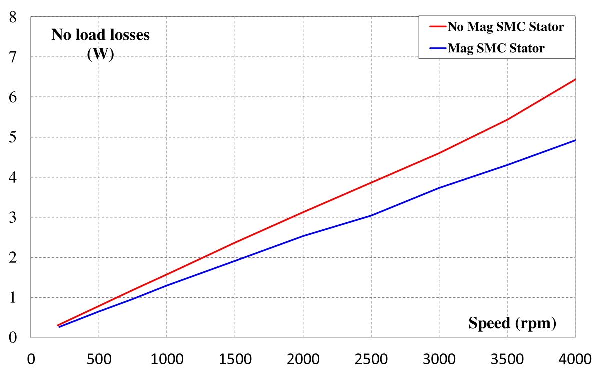

FIGURE 17. No-load test losses measurement for the proposed prototypes.

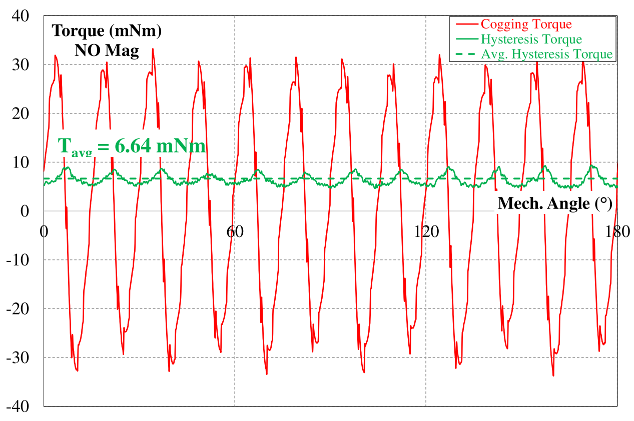

FIGURE 18. The cogging and hysteresis torque for the prototype with the non-magnetized SMC stator.

better, showing losses and torque 24 % lower than the prototype non-magnetized.

C. EFFECT OF MANUFACTURING MAGNETIZATION ON PROTOTYPES: TORQUE RIPPLE TEST

A second test that must be performed on prototypes is the evaluation of the cogging torque. In particular, contrary to what is done in the literature, here, a novel method that

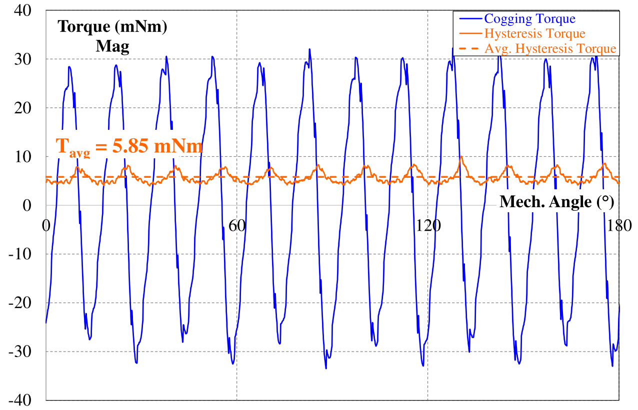

FIGURE 19. The cogging and hysteresis torque for the prototype with the magnetized SMC stator.

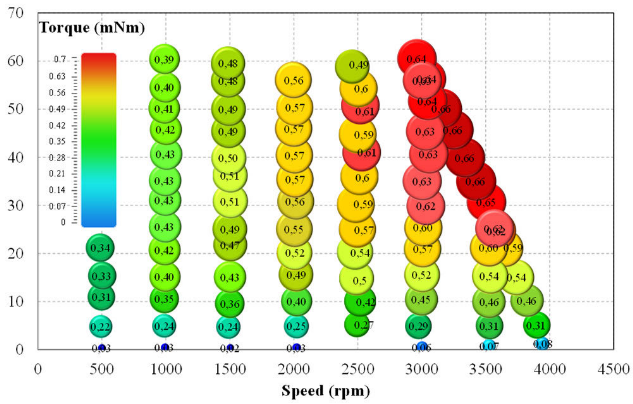

FIGURE 20. Measured data for efficiency map of the prototype with No Mag SMC Stator.

permits a fulfilling and accurate assessment of different contributions, which means hysteresis contribution and cogging torque contribution, was used, as previously described in [32]. Fig. 18 and Fig. 19 showed results in terms of cogging torque and hysteresis in the two prototypes.

The high cogging torque value (Fig. 18 and Fig. 19) is due to the absence of the polar expansions, and it is not only a drawback: when operated at high speed, the machine shows a cogging torque frequency well outside the audio range. The torque ripple should also be negligible due to the rotor inertia. An advantage of this topology is a wide difference between the L_d and L_q inductance, which facilitates the use in conjunction with a Field Oriented Control.

Considering individual results on material behavior, especially on the permeability values, it was attended a high value in cogging torque peak-peak value for the machine having the stator with magnetized SMC. Conversely, a very low difference between the two stators was measured. Also, hysteresis torque was measured where the non-magnetized prototype shows a value of about 12% higher, confirming the higher iron losses.

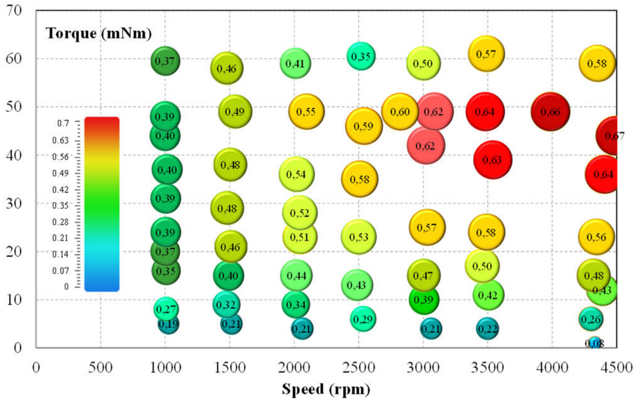

FIGURE 21. Measured data for efficiency map of the prototype with Mag SMC Stator.

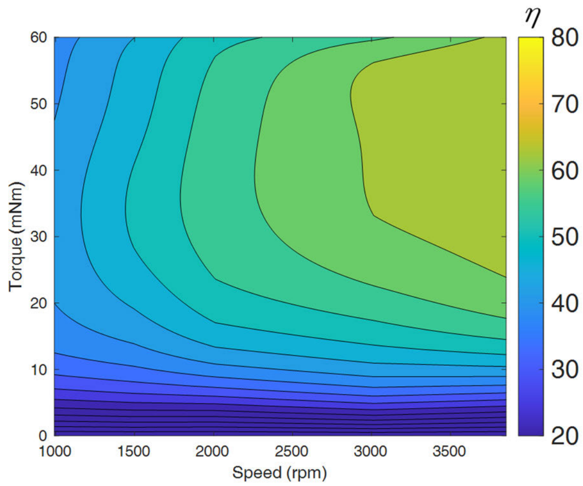

FIGURE 22. Efficiency map of the prototype with No Mag SMC Stator obtained by post-processing activity.

D. EFFECT OF MANUFACTURING MAGNETIZATION ON PROTOTYPES: LOAD TEST

The third test that must be conducted on prototypes regards evaluating the machine response if a load is applied. The load tests are performed using the electronic conversion device. The inverter's control is adjusted to obtain several points and works until the rated condition is reached. Repeating the measurement at the same setup and similar intervals is difficult. For these reasons, the obtained results for the two stators are slightly different in measured intervals of the efficiency map, as shown in Fig. 20 and Fig. 21. The highest efficiency value, 67%, is obtained for the Mag SMC stator prototype. On the other hand, the No Mag SMC stator machine seems to show a larger area with efficiency values higher than 60%. Considering the experimental data, the difference between the two proposed prototypes is around 1%. For this context, a detailed and deep assessment is adopted, using the post-processing activity based on the interpolation model of all experimental results. In this way, it is possible to get and improve results in the map following the typical efficiency trend. Such trends are built from experimental data for various speed intervals in order to fill the missing points.

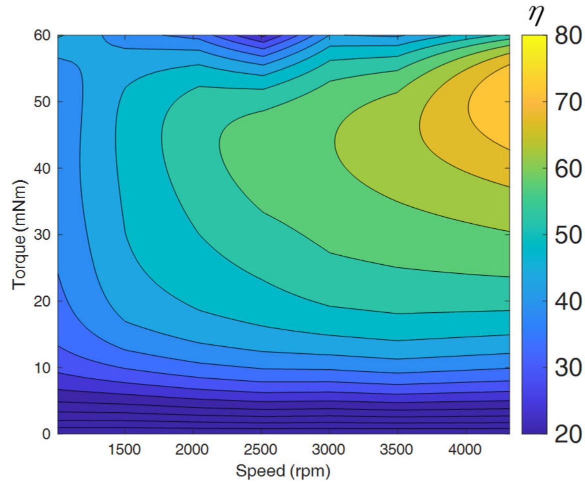

FIGURE 23. Efficiency map of the prototype with Mag SMC Stator obtained by post-processing activity.

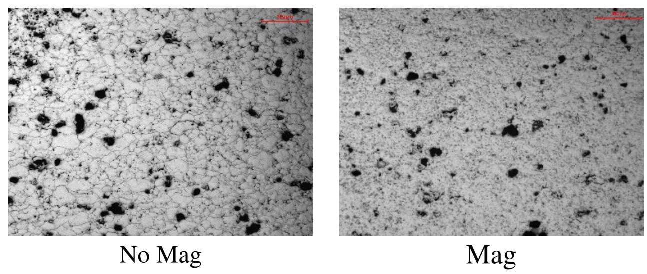

FIGURE 24. 5X magnification for for magnetized and no magnetized SMC materials during the compacted process.

As the experimental data are obviously not distributed along a "regular" matrix, it has been necessary to interpolate them first vertically and then horizontally in order to elaborate the detailed efficiency maps of Fig. 22 and Fig. 23 for the two tested machines, without and with magnetized SMC stator.

Such results validate the previous measure on SMC material, underlining that the machine having a magnetized stator performs better than a non-magnetized SMC stator, giving efficiencies of about 76 % and 67 %, respectively. On the other hand, the high efficiency for non-magnetized stator is preserved in a larger operative area torque-speed than magnetized stator. Furthermore, both values settle on the expected standard values for an Axial Flux Machine of similar size (60-70%). Additionally, even AFM realized using laminated steel can reach similar efficiency at equal rated torque; therefore, magnetizing SMC during the process permits the axial flux machine to be a good solution for fractional motors.

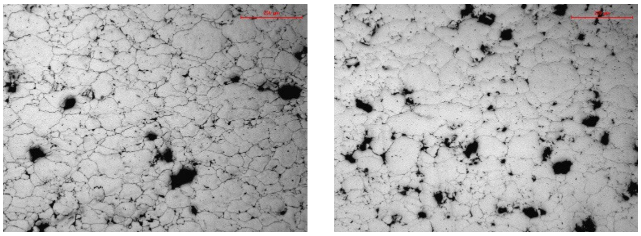

FIGURE 25. 10X magnification for for magnetized and no magnetized SMC materials during the compacted process.

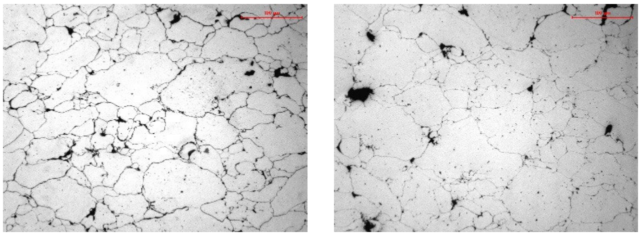

FIGURE 26. 20X magnification for for magnetized and no magnetized SMC materials during the compacted process.

E. EFFECT OF MANUFACTURING MAGNETIZATION ON PROTOTYPES: MICROSTRUCTURE ANALYSIS

Optical microscope MEF4, Leica (magnifications 20X→ marker 100 μm,10X→ marker 200 μm 5X→ marker 300 μm) has been used to observe the metallographic behavior on the scarps of the toroidal samples. The metallographic etching was performed using a Nital 2% solution containing nitric acid in 2% and etilic alcool. Such etching is commonly used to reveal microstructural features in iron base alloys.

In Fig. 24, the lower magnifications are shown for No Mag SMC and Mag SMC materials. The microstructure in the case of No Mag SMC seems more porous, while the Mag SMC show a more compacted structure and minor numbers of macroporous. The oriented structure of particles due to magnetization during the process is not possible to observe at 5X; for this reason, Fig. 25 is shown. The magnetization effect does not orient or align the particles but improves the compaction and reduces the intergranular space and distance, as observed for magnetized SMC materials. A further magnification, reported in Fig. 26, confirms a better consolidation and more dense structure for magnetized SMC materials observing the intergranular lines that are barely noticeable.

F. EFFECT OF MANUFACTURING MAGNETIZATION ON PROTOTYPES: FINAL DISCUSSION

SMC materials, thanks to the magnetization during compaction, lead to a reduction in iron losses. Up to today, this behaviour has still not been totally explained. Nevertheless, the most widely accepted hypothesis suggested that:

- The attractive force between the ferromagnetic object concurs, along with the pressure applied by the press, in increasing the total pressure applied during the compaction phase;
- A certain powder orientation can be reached thanks to the tendency of the particles to dispose of themselves in a minimum reluctance condition. This, in turn, can lead to an increase in grain displacement and orientation ordering, reducing the inner demagnetizing fields;

Particularly, considering the metallographic analysis results, seems that actually exists a pressure effect that affects the microstructure. The observation of magnetic domains by magneto-optical microscopy, based on the Kerr effect, can be considered in future to confirm these hypotheses.

V. CONCLUSION

In this work, the effect of the usage of specifically prepared SMC for a stator application in AFM was studied. In particular, SMC stators were studied, considering the effect of applying magnetization during the compaction. Both magnetized and non-magnetized stators lead to very promising results. Mainly, the higher permeability values were obtained by the magnetized SMC; moreover, iron losses can be reduced up to 15 % for 400 Hz@1T, increasing the energetic aspects.

Conversely, cogging measurements lead to similar values in the two prototypes. Regarding efficiency, maps showed a higher result for the magnetized stator, while the stator non-magnetized permit to work in a higher efficiency speed-torque range observing through post-processing activity.

The main limitation lies in the maximum applied pressure on the specifically produced mold of 500 MPa.

In the next future, an assessment of the relationship between experimental results and FEM simulation will be performed with the aim to enhance the AFM design.

Due to the limitations of the particular mold, the used approach of 500 MPa instead of 800 MPa will be reconsidered.

ACKNOWLEDGMENT

The part of the research activities developed by Emir Pošković was carried out within the framework of Ministerial Decree no. 1062/2021 and received funding from the FSE REACT-EU-PON Ricerca e Innovazione 2014-2020. This manuscript reflects only the views and opinions of the authors, neither the European Union nor the European Commission can be considered responsible for them.

REFERENCES

[1] S. Kahourzade, A. Mahmoudi, H. W. Ping, and M. N. Uddin, "A comprehensive review of axial-flux permanent-magnet machines," *Can. J. Electr. Comput. Eng.*, vol. 37, no. 1, pp. 19–33.

[2] N. Rahim, H. Ping, and M. Tadjuddin, "Design of an in-wheel axial flux brushless DC motor for electric vehicle," in *Proc. Int. Forum Strategic Technol.*, Ulsan, South Korea, Oct. 2006, pp. 16–19.

[3] P. J. Masson, M. Breschi, P. Tixador, and C. A. Luongo, "Design of HTS axial flux motor for aircraft propulsion," *IEEE Trans. Appl. Supercond.*, vol. 17, no. 2, pp. 1533–1536, Jun. 2007.

[4] S. A. Kim, S. I. Byun, H. K. Jeon, and Y. H. Cho, "Characteristics comparison of a conventional and novel stator structure of axial flux permanent magnet motor for cooling fan drive system," in *Proc. IEEE Int. Electric Mach. Drives Conf. (IEMDC)*, Coeur d'Alene, ID, USA, May 2015, pp. 154–159.
[5] B. Cheng, G. Pan, and Z. Mao, "An axial flux double-rotor counter-rotating permanent magnet machine for underwater vehicles," in *Proc. IEEE 8th Int. Conf. Adv. Power Syst. Autom. Protection (APAP)*, Xi'an, China, Oct. 2019, pp. 1304–1308.
[6] A. Di Gerlando, G. Foglia, M. F. Iacchetti, and R. Perini, "Axial flux PM machines with concentrated armature windings: Design analysis and test validation of wind energy generators," *IEEE Trans. Ind. Electron.*, vol. 58, no. 9, pp. 3795–3805, Sep. 2011.
[7] A. S. Holmes, G. Hong, and K. R. Pullen, "Axial-flux permanent magnet machines for micropower generation," *J. Microelectromech. Syst.*, vol. 14, no. 1, pp. 54–62, Feb. 2005.
[8] L. Shao, R. Navaratne, M. Popescu, and G. Liu, "Design and construction of axial-flux permanent magnet motors for electric propulsion applications—A review," *IEEE Access*, vol. 9, pp. 158998–159017, 2021.
[9] J. F. Gieras, R. J. Wang, and M. J. Kamper, *Axial Flux Permanent Magnet Brushless Machines*. Dordrecht, The Netherlands: Springer, 2008.
[10] F. Franchini, E. Poskovic, L. Ferraris, A. Cavagnino, and G. Bramerdorfer, "Application of new magnetic materials for axial flux machine prototypes," in *Proc. IEEE Int. Electric Mach. Drives Conf. (IEMDC)*, Miami, FL, USA, May 2017, pp. 1–6.
[11] W. Deng and S. Zuo, "Axial force and vibroacoustic analysis of external-rotor axial-flux motors," *IEEE Trans. Ind. Electron.*, vol. 65, no. 3, pp. 2018–2030, Mar. 2018.
[12] P. Ramesh and N. C. Lenin, "High power density electrical machines for electric vehicles—Comprehensive review based on material technology," *IEEE Trans. Magn.*, vol. 55, no. 11, pp. 1–21, Nov. 2019.
[13] A. T. de Almeida, F. J. T. E. Ferreira, and G. Baoming, "Beyond induction motors—Technology trends to move up efficiency," *IEEE Trans. Ind. Appl.*, vol. 50, no. 3, pp. 2103–2114, May 2014.
[14] P. Eklund and S. Eriksson, "The influence of permanent magnet material properties on generator rotor design," *Energies*, vol. 12, no. 7, p. 1314, Apr. 2019.
[15] E. Poskovic, L. Ferraris, F. Carosio, F. Franchini, and N. Bianchi, "Overview on bonded magnets realization, characterization and adoption in prototypes," in *Proc. 45th Annu. Conf. IEEE Ind. Electron. Soc.*, vol. 1, Lisbon, Portugal, Oct. 2019, pp. 1249–1254.
[16] R. Madhavan and B. G. Fernandes, "Axial flux segmented SRM with a higher number of rotor segments for electric vehicles," *IEEE Trans. Energy Convers.*, vol. 28, no. 1, pp. 203–213, Mar. 2013.
[17] D.-K. Lim, Y.-S. Cho, J.-S. Ro, S.-Y. Jung, and H.-K. Jung, "Optimal design of an axial flux permanent magnet synchronous motor for the electric bicycle," *IEEE Trans. Magn.*, vol. 52, no. 3, pp. 1–4, Mar. 2016.
[18] S. Berndl and A. Kleimaier, "Influence of the U-core geometry on the torque behavior of scalable axial flux motors," in *Proc. Int. Symp. Power Electron., Electr. Drives, Autom. Motion (SPEEDAM)*, Sorrento, Italy, Jun. 2022, pp. 466–472.
[19] R. Al Zaher, S. de Groot, H. Polinder, and P. Wieringa, "Comparison of an axial flux and a radial flux permanent magnet motor for solar race cars," in *Proc. XIX Int. Conf. Electr. Mach.*, Rome, Italy, Sep. 2010, pp. 1–6.
[20] G. R. Bruzinga, A. J. S. Filho, and A. Pelizari, "Analysis and design of 3 kW axial flux permanent magnet synchronous motor for electric car," *IEEE Latin Amer. Trans.*, vol. 20, no. 5, pp. 855–863, May 2022.
[21] X. Wang, X. Zhao, P. Gao, and T. Li, "A new parallel magnetic circuit axial flux permanent magnet in-wheel motor," in *Proc. 24th Int. Conf. Electr. Mach. Syst. (ICEMS)*, Gyeongju, South Korea, Oct. 2021, pp. 1107–1111.
[22] B. Vicenzi, K. Boz, and L. Aboussouan, "Powder metallurgy in aerospace-fundamentals of PM processes and examples of applications," *Acta Metallurgica Slovaca*, vol. 26, no. 4, pp. 144–160, Dec. 2020.
[23] E. A. Périgo, B. Weidenfeller, P. Kollár, and J. Füzer, "Past, present, and future of soft magnetic composites," *Appl. Phys. Rev.*, vol. 5, no. 3, Jul. 2018, Art. no. 031301.
[24] A. Schoppa and P. Delarbre, "Soft magnetic powder composites and potential applications in modern electric machines and devices," *IEEE Trans. Magn.*, vol. 50, no. 4, pp. 1–4, Apr. 2014.
[25] E. Pošković, F. Franchini, L. Ferraris, E. Fracchia, J. Bidulska, F. Carosio, R. Bidulsky, and M. Actis Grande, "Recent advances in multi-functional coatings for soft magnetic composites," *Materials*, vol. 14, no. 22, p. 6844, Nov. 2021.
[26] X. Wang, Z. Wan, M. Zhao, and W. Xu, "Performance of an axial flux hybrid excitation motor with SMC for HEVs," in *Proc. IEEE Int. Conf. Appl. Supercond. Electromagn. Devices (ASEMD)*, Tianjin, China, Oct. 2020, pp. 1–2.
[27] G. S. Liew, N. Ertugrul, W. L. Soong, and D. B. Gehlert, "Analysis and performance evaluation of an axial-field brushless PM machine utilising soft magnetic composites," in *Proc. IEEE Int. Electric Mach. Drives Conf.*, Antalya, Turkey, May 2007, pp. 153–158.
[28] L.-O. Pennander, E. Gutowski, and L. Lackner, "Design and implementation of SMC components for an automotive electric water pump," in *Proc. WorldPM*, Beijing, China, Sep. 2018, pp. 1–7.
[29] E. Pošković, F. Franchini, and L. Ferraris, "The magnetization effect on soft magnetic composite prepared stators of axial flux motors," in *Proc. IEEE Energy Convers. Congr. Expo. (ECCE)*, Detroit, MI, USA, Oct. 2022, pp. 1–7.
[30] E. Pošković, F. Carosio, L. Ferraris, F. Franchini, and M. A. Grande, "Processo per la produzione di materiali magnetici nanorivestiti," Italy National Patent 102 021 000 026 681, Oct. 18, 2021.
[31] E. Pošković, F. Carosio, L. Ferraris, F. Franchini, and M. A. Grande, "Process for the production of nano-coated ferromagnetic materials," PCT Patent WO 2 023 067 471, Apr. 27, 2023.
[32] L. Ferraris, F. Franchini, and E. Poskovic, "Improvements in the hysteresis and cogging evaluation with an innovative methodology," in *Proc. Int. Conf. Electr. Mach. (ICEM)*, Alexandroupoli, Greece, Sep. 2018, pp. 250–256.

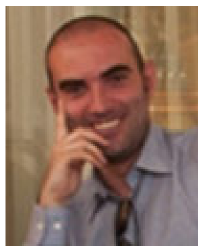

EMIR POŠKOVIĆ (Member, IEEE) was born in Sarajevo, Bosnia and Herzegovina. He received the B.S. and M.Sc. degrees in electrical engineering from the Polytechnic University of Turin, in 2006 and 2008, respectively, and the Ph.D. degree in electrical energy engineering from the University of Padova, in 2020.

He is currently an Assistant Professor with the Energy Department "G. Ferraris," Politecnico di Torino, and a Key Researcher with the Magnetic Characterization Laboratory, Politecnico di Torino, Alessandria Campus. His special fields of interest included soft and hard magnetic materials, electrical machines, and alternative and renewable energy (micro-hydro, fuel cell, and PV-photovoltaic). He has published about 80 scientific papers in conference proceedings and technical journals.

Dr. Pošković was a recipient of two best paper awards. He is a reviewer of several international journals and conferences.

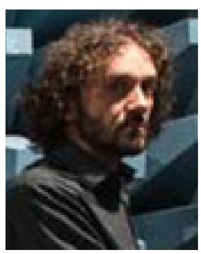

FAUSTO FRANCHINI received the B.S. degree in electrical engineering from Politecnico di Torino, Alessandria, Italy, in 2003. Since 2004, he has been a Technician with the Electrical Engineering Laboratory, Politecnico di Torino, where he has been responsible for the laboratory, since 2007. His fields of research interests include electromagnetic metrology, electromagnetic compatibility, data acquisition, control, and automation.

ELISA FRACCHIA received the bachelor's degree in mechanical engineering and the master's degree in material science and engineering, in 2017. She is currently pursuing the Ph.D. degree with the Department of Management and Production Engineering (DIGEP), Politecnico di Torino.

She subsequently worked as a Research Fellow, until 2021. She is affiliated with the Consorzio Interuniversitario Nazionale per la Scienza e Tecnologia dei Materiali (INSTM). She is a Secretary with the Light Metals Division, Italian Association of Metallurgy. Her research interests include light alloys, particularly aluminium alloys, for wrought and casting purposes. The research group, where she works deals with the study and characterization of automotive components and the design of new challenging alloys.

SILVIO VASCHETTO (Senior Member, IEEE) received the M.Sc. and Ph.D. degrees in electrical engineering from Politecnico di Torino, Turin, Italy, in 2007 and 2011, respectively.

He then joined the ABB IEC LV Motors Technology Center, Vittuone, Italy, as a Research and Development Engineer. From 2012 to 2014, he was with Magna Electronics, Italy, as an Electromagnetic Simulation and Motor Design Engineer. He is currently an Associate Professor with the Energy Department "G. Ferraris," Politecnico di Torino. His research interests include electromagnetic design, thermal design, and the energetic behavior of electrical machines for transportation and high-performance applications. He is an Associate Editor of IEEE Transactions on Industry Applications and IEEE Transactions on Energy Conversion and a Special Issues Editor of *IET Electric Power Applications*.

LUCA FERRARIS (Member, IEEE) received the M.S. degree in electrical engineering from Politecnico di Torino, Turin, Italy, in 1992.

In 1995, he joined the Department of Electrical Engineering (now the Energy Department), Politecnico di Torino, where he is currently an Associate Professor of electrical machines and drives and coordinates the experimental activities with Electric and Electromagnetic Laboratories. He also leads the activities of the Magnetic Characterization Laboratory, Alessandria Campus. He has published more than 140 technical papers in conference proceedings and technical journals. His research interests include the energetic behavior of machines, innovative magnetic materials for electromagnetic devices, electrical traction, electromagnetic compatibility, and renewable energies.

ALBERTO TENCONI (Senior Member, IEEE) received the M.Sc. and Ph.D. degrees in electrical engineering from Politecnico di Torino, Turin, Italy, in 1986 and 1990, respectively.

From 1988 to 1993, he was with the Electronic System Division, FIAT Research Center, where he was engaged in the development of electrical vehicle drive systems. Then, he joined the Department of Electrical Engineering (now the Energy Department), Politecnico di Torino, where he is currently the Head of the Department. His research activity is documented by more than 200 papers published in international journals and international conferences. He has participated, both as a Designer and a Scientist responsible for many national and European research programs. His current research interests include electric machines, power converters, and drives for transportation electrification. He is a reviewer of international journals and has been an Associate Editor of IEEE Transactions on Industrial Electronics.